Article

Not peer-reviewed version

Use of Cyclodextrins for the Recognition of a Highly Toxic and Explosive Environment: A Study Based on Partial Molar Volumes, Compressibilities and Spectroscopic Techniques

Mauricio Maldonado , Edilma Sanabria , Diana M. Galindres-Jimenez , Carmen M. Romero , Miguel A. Esteso *

Posted Date: 11 November 2025

doi: 10.20944/preprints202511.0705.v1

Keywords: 4-nitrophenol; cyclodextrins; host-guest complexes; pollutant; partial molar volumes; compressibilities

 doi:10.20944/preprints202511.0705.v1

Article

Use of Cyclodextrins for the Recognition of a Highly Toxic and Explosive Environment: A Study Based on Partial Molar Volumes, Compressibilities and Spectroscopic Techniques

Mauricio Maldonado [1], Edilma Sanabria [2], Diana M. Galindres-Jimenez [3,4], Carmen M. Romero [1] and Miguel A. Esteso [3,5,*]

[1] Departamento de Química, Facultad de Ciencias, Universidad Nacional de Colombia, Sede Bogotá, Carrera 30 No. 45-03, Bogotá 111311, Colombia
[2] Grupo GICRIM, Programa de Investigación Criminal, Universidad Manuela Beltrán, Avenida Circunvalar No. 60-00, 111321, Bogotá, Colombia
[3] Faculty of Health Sciences, Universidad Católica de Ávila, Calle Los Canteros s/n, 05005 Ávila, Spain
[4] Grupo de Investigación en Ciencias y Educación (ICE), Facultad de Ingeniería, Universidad de América, Carrera 1 No. 20-53, 111711 Bogotá, Colombia
[5] U.D. Química Física, Universidad de Alcalá, 28805 Alcalá de Henares, Spain
* Correspondence: mangel.esteso@ucavila.es

Abstract

The aim of this work was to find an alternative method for the isolation and inactivation of 4-nitrophenol in aqueous solution by complexing it with cyclodextrins. For that, the inclusion complex between cyclodextrins and 4-nitrophenol (4-NP) was investigated using UV-Visible and ^{1}H-NMR spectroscopies. These results allowed us to observe the existence of a strong interaction between (4-NP) and 2-hydroxypropyl-β-cyclodextrin (2-HP-β-CD). Moreover, other specific properties of this complex in solution were also analysed. Thus, apparent partial molar volumes, apparent partial molar adiabatic compressibilities, partial molar volumes of transfer and interaction and intrinsic volumes were determined, allowing to evaluate the characteristics of the complex formed.

Keywords: 4-nitrophenol; cyclodextrins; host-guest complexes; pollutant; partial molar volumes; compressibilities

1. Introduction

Numerous pollutants are released into the atmosphere, water bodies, and soil everyday as a result of uncontrolled human activities. Among these pollutants, nitrophenols (NPs) and its various derivatives constitute an important environmental problem because they are highly toxic for humans and many other animal and plant species. Consequently, soils and water of seas, lakes, streams and underground currents contaminated by these compounds have negative effects on all ecosystems directly or indirectly related to them [1]; they are substances phytotoxic to the planet [2].

They have a high stability and solubility in water, so they can reduce the concentration of dissolved oxygen in natural waters, affecting aquatic ecosystems [3]. Moreover, they are not biodegradable and have a high presence as a result of their use by various industries (drugs, dyes, explosives, plasticizers, pesticides, artificial colors and petrochemicals), as well as because they are produced by the degradation of fungicides and insecticides used in agriculture, such as parathion and nitrofen [2–4], by the burning of biomass and by traffic emissions, among others daily activities [5]. Due to their relative volatility, NPs are distributed in gaseous form and are present in urban, suburban, rural, coastal and mountainous areas. Furthermore, they can be formed in the atmosphere

 doi:10.20944/preprints202511.0705.v1

by oxidation of phenol in the presence of OH and NO_2 radicals during the day or at night in the presence of NO_2 and NO_3 [5]. A study carried out in 2012 by the University of Chile revealed that, for the period between august and October, 4-nitrophenol was present in 72.7% of the cases when dew droplets were analysed. Currently, there are no similar studies, but this percentage is expected to have increased because its production has been continuous and, as previously indicated, this compound is not biodegradable [6].

As a consequence of their biotoxicity, these noxious pollutants cause damage to different organs in animals and humans. In the latter case, NPs can cause mutagenic effects and cancer [7,8]; even at very low concentrations [1], are potential teratogens and mutagens [4], and can affect the central nervous system, blood cells and organs such as the kidney and liver [2]. Symptoms of acute intake include nausea, cyanosis, dizziness, skin irritation, methemoglobinemia, drowsiness, and severe headaches [4]. In particular, 4-nitrophenol (4-NP) has been classified by the USEPA (United States Environmental Protection Agency) as high-priority hazardous pollutant being prohibited its use [9]. It is associated with oxidative stress, inflammation, apoptosis in different tissues [10] and cancer [11].

Some techniques have been proposed to recognize and remove NPs from contaminated water, air or soil. These include detection using an electrochemical sensor [12]; selective separation and enrichment of nitrophenols with a printed monolith [13]; formation of an inclusion complex with bis-8-hydroxyquinolinium zinc-2,6-pyridinedicarboxylate [14]; and a spray tower plasma-reactor in a spatial post-discharge configuration for remote pollutant treatment [15], among others. Macrocycles have also been used for this purpose. For example, phthalocyanines [16,17], tetrapyrrolic macrocycles [18] and cobalt-porphyrin complexes have been tested [19], among others.

Continuing this line, this research shows the findings made in the recognition of (4-NP) (Figure 1a) with 2-hydroxypropyl-β-cyclodextrin (2-HP-β-CD) at 298.15 K. This cyclodextrin has the advantage of being water-soluble [20], having low toxicity, not being hygroscopic, chemically stable and easily separable. All these properties favor its use in the chemical, pharmaceutical [21], food, agricultural and environmental industries [22,23].

(2-HP-β-CD) is a cyclic oligosaccharide containing seven D-glucopyranose units linked by (1,4)-glycosidic bonds. It has a hydrophobic inner cavity where water-insoluble molecules can be accommodated. The exterior of this macrocycle is hydrophilic (Figure 1b). This structure facilitates the formation of inclusion complexes with different hydrophobic guests which, thus, enhance their solubility [24].

The objective of this work is to find an alternative and effective method to complex 4-NP in water, in order to isolate and inactivate it. For this purpose, the host-guest-type complex {(2-HP-β-CD)/(4-NP)} was obtained and its structural characteristics evaluated by using NMR, FT-IR, masses and UV-Vis spectroscopies. In addition, apparent molar volumes and isentropic compressibilities of this complex were determined in aqueous solutions, at different concentrations of both components, and analyzed with respect to the values corresponding to the isolated components, (4-NP) and (2-HP-β-CD). All the experiments were carried out at 298.15 K.

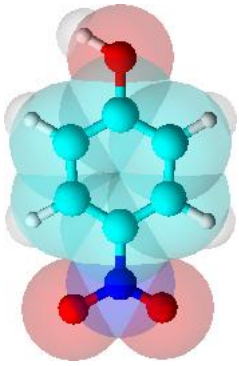

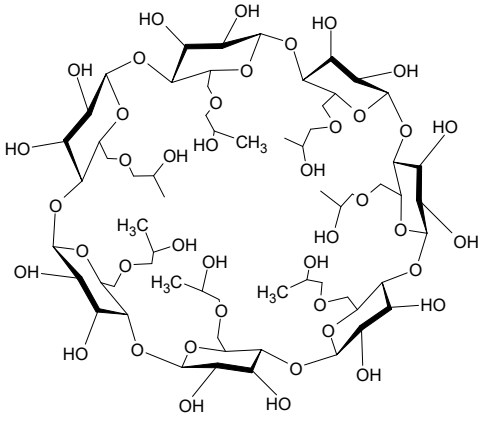

 doi:10.20944/preprints202511.0705.v1

a b

Figure 1. a) 4-nitrophenol (4-NP) structure; b) 2-hydroxypropyl-*β*-cyclodextrin (2-HP-*β*-CD) structure.

2. Results and Discussion

2.1. Spectroscopic Studies

As mentioned above, the interaction between 4-nitrophenol (4-NP) and 2-hydroxypropyl-*β*-cyclodextrin (2-HP-*β*-CD) in water was investigated by spectroscopic techniques. As a preliminary test, the molecular interaction was studied by UV-Vis spectroscopy. First, the spectrum of 4-NP in aqueous solution was analysed (line b in Figure 2), which showed a main absorption band at a wavelength at 325 nm and another secondary absorption band at 420 nm. Subsequently, the spectrum of an equimolar mixture of {(4-NP) + (2-HP-*β*-CD)} in aqueous solution was analysed (line c in Figure 2), observing a hyperchromic effect of the 4-nitrophenol band at 420 nm. It is worth nothing that this cyclodextrin does not exhibit absorption in this region of the UV-Visible spectrum (line a in Figure 2), so the aforementioned hyperchromatic effect must be due to the interaction of (4-NP) with the cyclodextrin. Thus, this behavior, resulting from the mixture of the two components, indicates the existence of a clear interaction between them, possibly by the formation of a host-guest type inclusion complex.

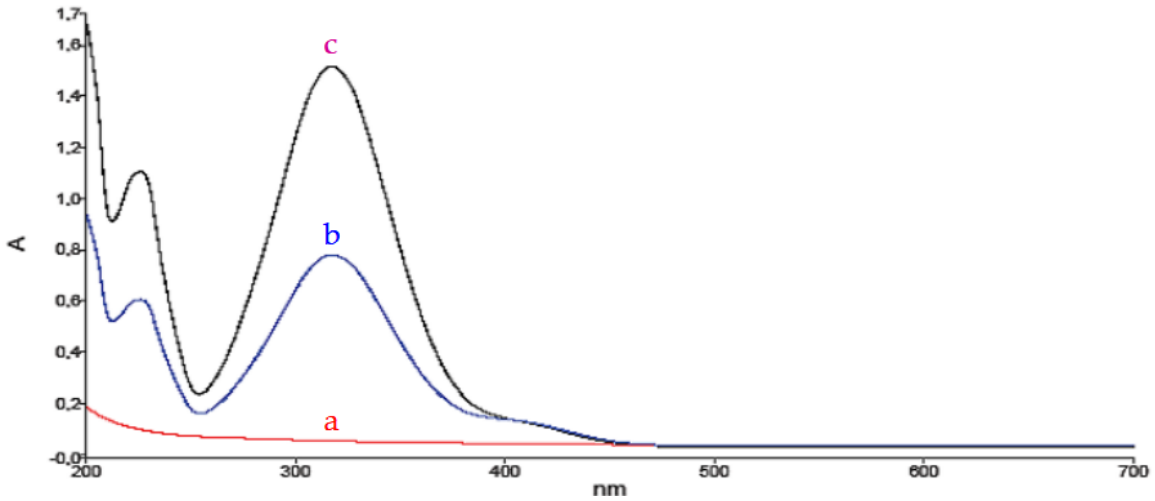

Figure 2. UV-visible spectra of: a) 2-hydroxypropyl-β-cyclodextrin (red line ▬), b) 4-nitrophenol (blue line ▬) and c) the equimolar mixture of both components (purple line ▬).

To confirm the interaction between (4-NP) and (2-HP-*β*-CD), it was decided to study the system using the NMR technique. For this purpose, individual ^{1}H-NMR spectra of both (4-NP) and (2-HP-*β*-CD) were obtained in deuterated water. The ^{1}H-NMR spectrum of (4-NP) in D_2O (green line in Figure 3) shows two characteristic signals: the first signal, corresponding to the protons in the *ortho* position with respect to the nitro group, at 8.03 ppm, and the second signal, corresponding to the protons in the *meta* position with respect to the nitro group, at 6.83 ppm. Once the characteristic signals of (4-NP) were established, the spectrum of the equimolar mixture of this with (2-HP-*β*-CD) was analyzed (blue line in Figure 3). This spectrum shows a shift in the signal of the protons from the *meta* position with respect to the nitro group, which appears at 6.90 ppm, while the protons in the *ortho* position do not show an appreciable shift.

 doi:10.20944/preprints202511.0705.v1

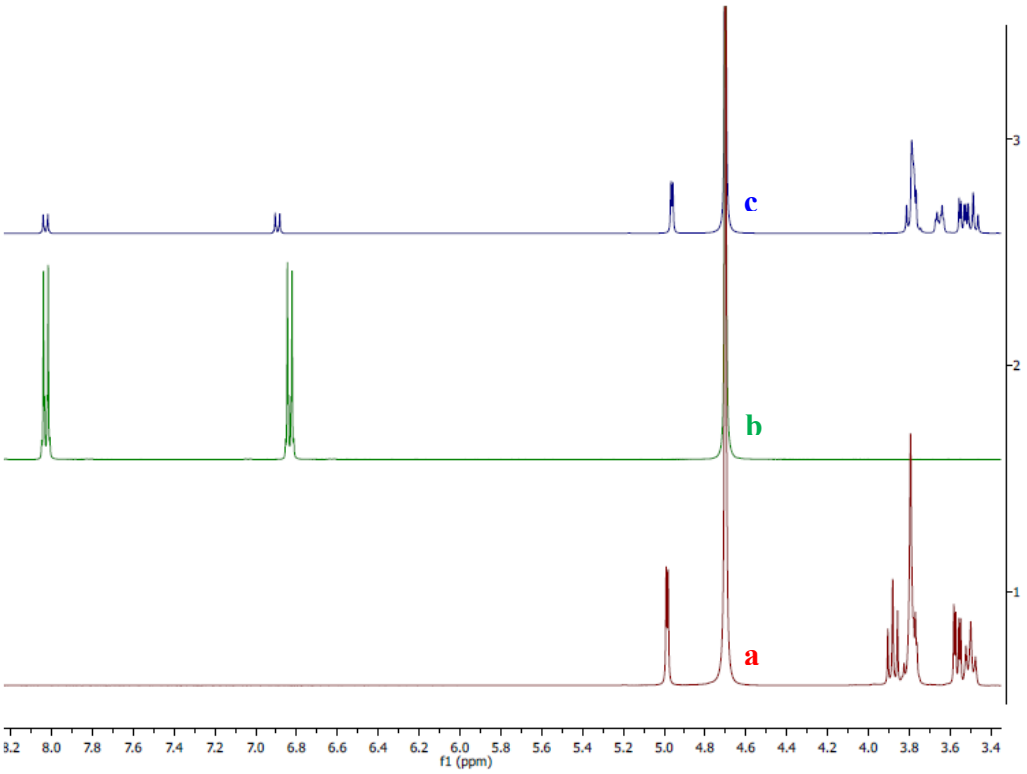

Figure 3. Comparative ^{1}H-NMR in D_2O: a) 2-hydroxypropyl-*β*-cyclodextrin (red line), b) 4-nitrophenol (green line) and c) the complex {(4-NP) + (2-HP-*β*-CD)} (blue line)

Another interesting aspect is the observed shift in the (2-HP-*β*-CD) signals (red line), specifically the triplet signal at 3.90 ppm. As it can be seen in the spectrum of the mixture (blue line), this signal undergoes a notable change; first, it shows a shift to 3.83 ppm, and also its multiplicity is significantly affected. These results suggest that the molecular interaction occurs between the OH functional group of (4-NP) and the polar cavity of (2-HP-*β*-CD), possibly through hydrogen-bonding interactions. It is important to note that when the same experiments were performed on a mixture with a higher stoichiometric ratio between (4-NP) and the CD (1:2 or 2:1), the same results were observed, allowing us to conclude that the host-guest complex is formed and, furthermore, that it has a 1:1 stoichimetry.

2.2. Analysis of Volumetric Properties

2.2.1. Binary Solutions

For binary solutions (solute + solvent), the apparent partial molar volume of the solute was obtained from experimental density data using equation (1):

$$V_{\phi} = \frac{M_2}{\rho} + \frac{1000\left(\rho_0 - \rho\right)}{m\rho\rho_0} \tag{1}$$

where ρ and ρ_0 represent the densities (in g·cm^{-3}) of the solution and the solvent, respectively, M_2 is the molar mass (in g·mol^{-1}) of the solute, and m is its molal concentration (mol·kg^{-1}). The apparent partial molal adiabatic compressibility, κ_{ϕ}, was calculated by using the following expression:

$$\kappa_{\phi} = \frac{M_2\beta_s}{\rho} + \frac{1000\left(\beta_s\rho_0 - \beta_s^0\rho\right)}{m\rho\rho_0} \tag{2}$$

where β_s^0 and β_s (in Pa^{-1}) correspond to the isentropic compressibility of the solvent and the solution, respectively, which were calculated from the Newton-Laplace equation:

 doi:10.20944/preprints202511.0705.v1

$$\beta_s = \frac{1}{\rho v^2} \tag{3}$$

v (in m·s^{-1}) being the speed of sound of the solvent or solution, as appropriate. Solvation numbers at infinitesimal ionic strength were obtained from β_s^0 and β_s using the Pasynski equation [25]:

$$n_h = \frac{n_1}{n_2}\left(1 - \frac{\beta_s}{\beta_s^0}\right) \tag{4}$$

2.2.1.1. 4-Nitrophenol Aqueous Solutions

Experimental values obtained for density and sound velocity are shown in Table 1S in the supplementary material.

The values for V_ϕ, β_s, κ_ϕ and n_h for aqueous solutions of (4-NP) at 298.15 K are shown in Table 1. The uncertainties in V_ϕ, β_s, κ_ϕ and n_h were calculated in accordance with the propagation uncertainty law.

Table 1. Values of V_ϕ, β_s, κ_ϕ and n_h of (4-NP) in water at T = 298.15 K and P = 101.3 kPa.

m (4-NP) /(mol·kg^{-1})	V_ϕ [a] /(cm^3·mol^{-1})	β_s [b] /(10^{-10} Pa^{-1})	κ_ϕ /(10^{-9} cm^3·mol^{-1}·GPa^{-1})	n_h
0.0049840	95.91	4.475	25.81	2.1
0.0060976	96.11	4.474	15.72	3.3
0.0071112	96.21	4.473	8.49	4.2
0.0076254	96.35	4.473	4.93	4.7
0.0090101	96.61	4.472	1.41	5.1
0.0099300	96.83	4.471	0.0798	5.3
0.010770	97.07	4.471	-2.27	5.6
0.011775	97.27	4.470	-2.87	5.7
0.013223	97.55	4.469	-3.69	5.8
0.013929	97.65	4.469	-3.87	5.8
0.015116	97.87	4.468	-4.58	5.9
0.020631	98.39	4.466	-3.73	5.8
0.030985	99.60	4.461	-1.54	5.6
0.042524	100.54	4.457	0.340	5.4
0.054795	101.29	4.452	2.07	5.3

[a] ρ_0 = 0.997047 g·cm^{-3}. [b] β_s^0 = 4.475·10^{-10} Pa^{-1}. Standard uncertainties are $u_r(m)$ = 0.0005 (max), $u_r(V_\phi)$ = 0.02 (max), $u_r(\beta_s)$ = 0.00014 (max), $u_r(\kappa_\phi)$ = 0.09 (max), $u(n_h)$ = 0.2 (max), $u(T)$ = 0.01K, $u(P)$ = 1 kPa.

In Figure 4 the values of V_ϕ for (4-NP) are plotted against its molal concentration. As it can be seen, two regions with quite different slopes are observed. This type of change in slope has been associated, in the case of hydrophobic solutes, with the formation of micellar aggregates [26]. In our case, this magg concentration may be associated with the formation of some type of aggregates from it. This concentration was determined using the Phillips method, based on the principle of searching for the concentration at which an abrupt change in a concentration-dependent property X occurs (i.e., $d^3X/dm^3 = 0$). In this case, the three properties, X = {V_ϕ, κ_ϕ and n_h}, were used [27,28] finding a mean value m_{agg} = 0.01504 ± 0.00003 mol·kg^{-1}. The plots of κ_ϕ and n_h *vs* the molal concentration are shown in Figures S1 and S2 in the supplementary material.

 doi:10.20944/preprints202511.0705.v1

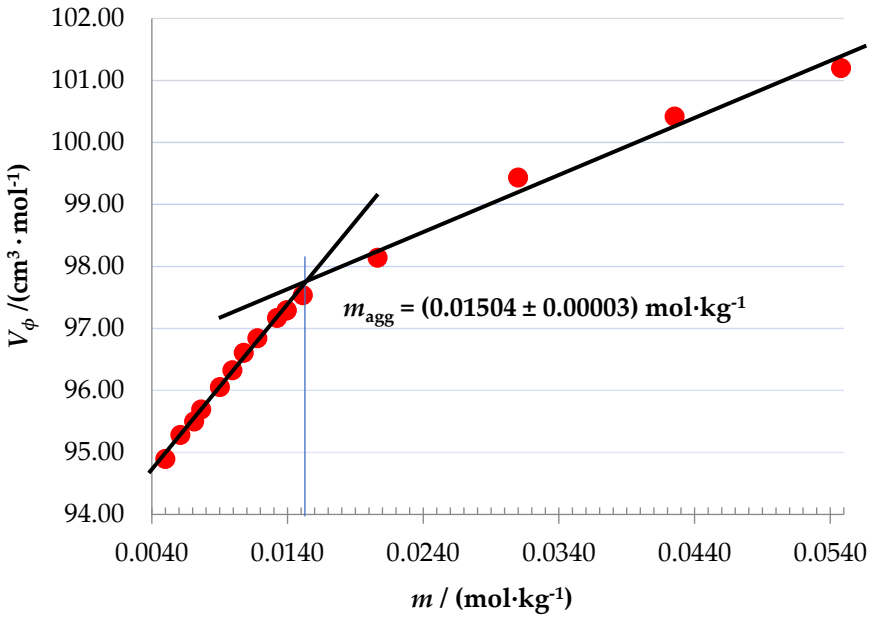

Figure 4. Apparent partial molal volume of 4-nitrophenol *vs* molal concentration in aqueous solution at T = 298.15K and P = 101.3 kPa.

The dependence of V_ϕ on m, in both intervals, was analyzed by linear weighted regression to a Redlich type equation [29], whose application to non-electrolyte solutions has been shown to be effective:

$$V_\phi = V_\phi^\infty + S_V\, m \tag{5}$$

being V_ϕ^∞ the limiting value at infinite dilution (which can be identified to the standard partial molar volume of the solute, V_2^0) and S_V an empirical parameter. The values found are collected in Table 2.

Table 2. Standard molar volumes, V_2^0, standard molar adiabatic compressibilities, κ_ϕ^0, and hydration numbers at infinite dilution, n_h^∞, together with the corresponding parameters of equations (5, 6 and 7), for aqueous solutions of (4-NP), (2-HP-β-CD) and the complex {(4-NP) + (2-HP-β-CD)}, at T = 298.15 K and P = 101.3 kPa.

System	V_2^0 /(cm³·mol⁻¹)	S_v /(cm³·kg·mol⁻²)	κ_ϕ^0 /(10⁻⁹ cm³·mol⁻¹·GPa⁻¹)	S_κ /(10⁻⁹ cm³·kg·mol⁻²·GPa⁻¹)	n_h^∞	b_n /(kg·mol⁻¹)
4-NP ($m < m_{agg}$)	94.83	204.26	3.30	-521.29	4.8	73.09
4-NP ($m > m_{agg}$)	96.54	90.61	-7.10	170.97	6.2	-16.63
2-HP-β-CD	849.44	1420.6	-0.90	1025.3	41.4	-82.67
{(4-NP)+(2-HP-β-CD)} complex	105.82	1316.7	23.32	1559.8	3.0	-122.8

Standard uncertainties are $u_r(V_2^0)$ = 0.02 (max), $u_r(\kappa_\phi^0)$ = 0.001 (max), $u(n_h^\infty)$ = 0.2 (max), $u(T)$=0.01K, $u(P)$ = 1 kPa.

It can be seen that S_V values are positive in both concentration regions (before and after m_{agg}), which means that the apparent partial molal volume of (4-NP) increases as its concentration in the solution increases. Since S_V is a measure of the solute-solute interactions taking place in the solution, these positive values indicate the presence of strong solute-solute interactions that are highest before the m_{agg} concentration is reached; this would justify the stabilization of complex solute-solute aggregation structures, with the resulting destructive overlap between their hydration spheres [30], leading to a decrease in the solvent structure around the solute molecules involved and, consequently producing a positive volume change.

 doi:10.20944/preprints202511.0705.v1

On the other hand, in Table 1 it can be seen that the isentropic compressibility of the solution, β_s, slighly decreases with the 4-NP concentration; i.e., that the compaction, under isentropic conditions, of the hydration spheres of the solute molecules becomes more difficult as the solute concentration increases and, therefore, the relative change in volume of the solution becomes more difficult.

In addition, in Table 1 and Figure S1, in the supplementary material, it can be ascertain that the apparent partial molal adiabatic compressibility, κ_ϕ, decreases strongly with the concentration of (4-NP), even reaching negative values, in the pre-aggregation region ($m < m_{agg}$). This behaviour, together with what was observed for the apparent partial molal volume and for the isentropic compressibility, leads to the conclusion that in this area of low 4-NP concentrations the solute-solute interaction is strong enough for aggregation structures (4-NP/4-NP) to appear, with the consequent destructive overlapping of the hydration shells, which leads to a loss of compressibility of the hydration spheres and, consequently, that the compaction capacity of the solution when pressure is applied is diminished. In the post-aggregation region ($m > m_{agg}$), the increase in the concentration of 4-NP leads to the structure-breaking effect of this solute on water structure, to build the corresponding hydration shell, managing to balance this effect, justifying the increasing of the apparent partial molal adiabatic compressibility observed when the 4-NP concentration increases [30].

The analysis of the variation of the apparent partial molal adiabatic compressibility with the concentration, to obtain the standard value, κ_ϕ^0, was carried out by fitting, using weighted least squares linear regression, the experimental values of κ_ϕ to the following equation:

$$\kappa_\phi = \kappa_\phi^\infty + S_K\, m \tag{6}$$

where κ_ϕ^∞ is the limiting value at infinite dilution (which can be identified to the standard molar adiabatic compressibility, κ_ϕ^0) and S_K is the empirical slope. The values found are collected in Table 2.

With respect to solvation numbers, these increase with the concentration of 4-NP in the pre-aggregation region ($m < m_{agg}$) while they decrease in the post-aggregation region ($m > m_{agg}$) (Figure S2 in Supplementary Materials). The dependence of the hydration numbers on the 4-NP concentration was analyzed through the linear equation:

$$n_h = n_h^\infty + b_n\, m \tag{7}$$

where n_h^∞ is the hydration number at infinite dilution and b_n is an experimental parameter. The values obtained are also shown in Table 2.

2.2.1.2. 2-Hydroxypropyl-β-Cyclodextrin Aqueous Solutions

Experimental values obtained for density and sound velocity are shown in Table 2S in the supplementary material.

The values for V_ϕ, β_s, κ_ϕ and n_h for aqueous solutions of (2-HP-β-CD) at 298.15 K are shown in Table 3. The uncertainties in V_ϕ, β_s, κ_ϕ and n_h were calculated according to the propagation uncertainty law.

Table 3. Values of V_ϕ, β_s, κ_ϕ and n_h of (2-HP-β-CD) in water at T = 298.15 K and P = 101.3 kPa.

m (2-HP-β-CD)/ (mol·kg^{-1})	V_ϕ [a] / (cm^3 · mol^{-1})	β_s [b] /(10^{-10} Pa^{-1})	κ_ϕ /(10^{-9} cm^3·mol^{-1}·GPa^{-1})	n_h
0.0036602	854.69	4.462	3.45	41.1
0.0043890	855.66	4.459	3.48	41.1
0.0051441	856.73	4.456	4.58	41.0
0.0059457	857.97	4.453	4.93	41.0
0.0066518	858.78	4.451	5.71	40.9
0.0073679	859.94	4.448	6.20	40.9

 doi:10.20944/preprints202511.0705.v1

0.0081319	860.91	4.445	7.48	40.7
0.0088565	861.98	4.442	8.15	40.7
0.0096982	863.23	4.439	8.93	40.6
0.0103320	864.27	4.437	10.1	40.5
0.0112429	865.35	4.434	10.7	40.5

[a] ρ_0 = 0.997047 g·cm^{-3}. [b] β_s^0 = 4.475·10^{-10} Pa^{-1}. Standard uncertainties are $u_r(m)$ = 0.0002 (max), $u_r(V_\phi)$ = 0.002 (max), $u_r(\beta_s)$ = 0.000032 (max), $u_r(\kappa_\phi)$ = 0.001 (max), $u(n_h)$ = 0.2 (max), $u(T)$ = 0.01K, $u(P)$ = 1 kPa.

It is worth highlighting the high values obtained for the apparent partial molar volumes of this cyclodextrin, which is consistent with what would be expected given that it is an organic compound with a high molar mass [31]. Furthermore, this apparent partial molar volume increases significantly with increasing solution concentration. Such increase in molal volume with increasing solute concentration in the solution has been associated with the existence of hydrophobic hydration of the solute [32,33] and in the case of apolar solutes (such as CDs), also to the existence of a strong solute-solute interactions which would favor the formation of dimeric structures of this cyclodextrin [34,35].

The dependence of V_ϕ on m was studied using the Redlich linear model:

$$V_\phi = V_2^0 + S_V\, m \tag{8}$$

V_2^0 being the standard molar volume of (2-HP-β-CD) and S_v is the slope.

This concentration dependence of V_ϕ on m is shown in Figure S3 of the supplementary material. As can be seen, a linear behavior is perfectly defined (R^2 = 0.9995). The values found are also collected in Table 2. Looking at these values in Table 2, it can be seen that the one found for S_V is much higher than that of V_2^0. If we take into account that V_2^0 corresponds to the limiting value at infinitesimal concentration, where practically only the solute-solvent interactions are felt, while S_V gives a measure of the solute-solute interactions, it can be inferred that for this solution the CD-CD interaction is more intense than the CD-water interaction [36,37], reinforcing what was stated before.

Regarding the apparent partial molal adiabatic compressibility, κ_ϕ, it is observed that it increases linearly with the concentration of the cyclodextrin in the solution (see Figure S4 in Supplementary Materials). Consequently, these experimental values were fitted to the linear equation (6) using a least squares regression, yielding a good correlation value (R^2 = 0.99). The values obtained for this fit are also shown in Table 2.

As it can be seen, the limiting value κ_ϕ^0 is negative. Considering that the molar compressibility is related to the structural changes that occur in the solvent as a result of the presence of the solute, negative values of κ_ϕ^0 are associated with a higher resistance of the solution against compression, compared to the pure solvent [33]. This increase in the adiabatic compressibility with increasing concentration can be justified by taking into account that (2-HP-β-CD) has hydroxypropyl groups on the outside of its molecule that enhance its hydrophilic character (being easy points of union with the surrounding water molecules) thus increasing its solubility in water; consequently, this cyclodextrin has a breaking effect on the structure of water.

The analysis of the dependence of the hydration number on the cyclodextrin concentration was performed using the linear equation (7). The values found are also shown in Table 2, and their behavior is shown in Figure S5 in the Supplementary Materials.

2.2.2. Ternary Aqueous Solutions

The ternary systems in solution (two solutes + solvent) were analyzed considering them as pseudo-binary systems; that is, as one solute (4-NP) dissolved in a mixed solvent (2HP-β-CD + water). However, the molalities of both solutes, 4-NP and 2-HP-β-CD, in the ternary solution are referred to the total amount of water present in said solution.

Experimental values of density and sound velocity obtained for these ternary systems are collected in Table 3S in the supplementary material.

 doi:10.20944/preprints202511.0705.v1

The apparent partial molar volumes, $V_{\phi,mix}$, were determined by using equation (1). In this case, ρ and ρ_0 denote the density values (in g·cm^{-3}) of the ternary solution (4-NP + 2HP-β-CD + water) and of the mixed solvent (2HP-β-CD + water) at the corresponding cyclodextrin concentration, respectively. The other variables, M_2 and m, are the molar mass (in g·mol^{-1}) and the molal concentration (in mol·kg^{-1}) of the 4-NP solution in the mixed solvent (2HP-β-CD + water).

In the same way, the apparent partial molal adiabatic compressibility values of the ternary solution, $\kappa_{\phi,mix}$, were calculated by means of the equation (2), being β_s and β_s^0 (in Pa^{-1}) the isentropic compressibility of the ternary solution (4-NP + 2HP-β-CD + water) and the mixed solvent (2HP-β-CD + water), respectively, calculated from equation (3). The rest of the variables have their usual meaning.

Finally, solvation numbers of 4-NP in these mixed solvent (2HP-β-CD + water) were determined from equation (4), and analysed as a function of the concentration.

The values found for $V_{\phi,mix}$, $\beta_{s,mix}$, $\kappa_{\phi,mix}$ and n_h for the {(4-NP)+(2-HP-β-CD)} aqueous system are shown in Table 4. The corresponding uncertainties were obtained from the propagation uncertainty law.

Table 4. Values of $V_{\phi,mix}$, $\beta_{s,mix}$, $\kappa_{\phi,mix}$ and n_h of (4-NP) in {(2-HP-β-CD) + water} mixed solvents at T = 298.15 K and P = 101.3 kPa.

m (4-NP)/ (mol·kg^{-1})	$V_{\phi,mix}$ / (cm^3·mol^{-1})	$\beta_{s,mix}$ / (10^{-10} Pa^{-1})	$\kappa_{\phi,mix}$ / (10^{-9} cm^3·mol^{-1} GPa^{-1})	n_h
0.0050504	112.45	4.461	31.16	2.3
0.0061101	113.95	4.458	32.72	2.2
0.0070596	115.03	4.455	34.61	2.1
0.0082791	116.97	4.452	36.49	1.9
0.0091986	117.95	4.449	37.94	1.8
0.010200	119.20	4.446	38.98	1.7
0.011245	120.28	4.444	40.43	1.6
0.012276	121.81	4.441	42.18	1.5
0.013487	123.66	4.438	44.22	1.3
0.014388	124.99	4.436	46.05	1.2
0.015680	126.46	4.432	47.99	1.0

Standard uncertainties are $u_r(m)$ = 0.001 (max), $u_r(V_{\phi,mix})$ = 0.009 (max), $u_r(\beta_s)$ = 0.000032 (max), $u_r(\kappa_{\phi,mix})$ = 0.0001 (max), $u(T)$ = 0.01K, $u(P)$ = 1 kPa.

Looking at Table 4 it can be seen that the value of $V_{\phi,mix}$ increases with the increase in the concentration of 4-NP, said increase being linear in the concentration range analyzed (Figure S6 in Supplementary Materials). This behaviour was analyzed by using the Redlich linear model (equation 8). The values found are given in Table 2.

As it can be seen, the S_v value is positive, indicating that the solute-solute interaction becomes increasingly stronger as the concentrations of the 4-NP and 2-HP-β-CD are higher as well. On the other hand, it can also be seen that these S_v values are quite high, although somewhat lower than the value presented by the pure cyclodextrin, which indicates that in these media the interactions between the solutes is more intense than with water.

On the other hand, the apparent partial molal adiabatic compressibility, $\kappa_{\phi,mix}$, also increases linearly with the concentration of 4-NP in the solution (see Figure S7 in the Supplementary Materials). This increase indicates that the solution becomes more compressible as the concentration of 4-NP increases, and its apparent molal volume also increases, indicating a breaking character on the water structure by 4-NP. Finally, the fact that the solvation numbers decrease with concentration ($b_n < 0$) (see Figure S8 in the Supplementary Materials) reinforces the idea that there is a structure-breaking

 doi:10.20944/preprints202511.0705.v1

effect on water, possibly favored by the destructive overlap between the solvation spheres of the solutes present [38].

2.2.2.1. Partial Molar Volumes of Transfer

Partial molar volumes of transfer, ΔV_ϕ, for 4-NP from water to the different (2-HP-β-CD + water) mixed solvents were calculated from the equation:

$$\Delta V_{\boldsymbol{\phi}} = V_{\boldsymbol{\phi,mix}} - V_{\boldsymbol{\phi}} \quad (9)$$

where the volume values are those collected in Tables 4 and 1, respectively. The values found are shown in Table 5.

Table 5. Partial molar volumes of transfer, ΔV_ϕ, for 4-NP from water to the different (2-HP-β-CD + water) mixed solvents at T = 298.15 K and P = 101.3 kPa.

m (4-NP) [a] / (mol·kg^{-1})	m (2-HP-β-CD) [a] / (mol·kg^{-1})	$V_{\phi,mix}$ / (cm^3·mol^{-1})	$V_{\phi,water}$ [b] / (cm^3·mol^{-1})	ΔV_ϕ / (cm^3 · mol^{-1})
0	0	105.82	94.83	10.99
0.0050504	0.0036602	112.45	95.86	16.59
0.0061101	0.0043890	113.95	96.08	17.87
0.0070596	0.0051441	115.03	96.27	18.76
0.0082791	0.0059457	116.97	96.52	20.45
0.0091986	0.0066518	117.95	96.71	21.24
0.010200	0.0073679	119.20	96.92	22.28
0.011245	0.0081319	120.28	97.12	23.16
0.012276	0.0088565	121.81	97.34	24.47
0.013487	0.0096982	123.66	97.58	26.08
0.014388	0.0103320	124.99	97.76	27.23
0.015680	0.0112429	126.46	98.03	28.43

[a] These molalities are calculated with respect to the amount of water present in the ternary solution. [b] These values, corresponding to pure 4-NP in water, were interpolated using the equation: {$V_{\phi,water}$ = 94.828 + 204.26 m} obtained in this work for said solute in that concentration range. Standard uncertainties are $u_r(m)$ = 0.0002 (max), $u_r(V_\phi)$ = 0.002 (max), $u(T)$ = 0.01K, $u(P)$ = 1 kPa.

It is observed that these transfer volumes are always positive and increase linearly with the concentration of the solutes (4-NP and 2-HP-β-CD) (see Figure S9 in the Supplementary Materials). This behavior can be explained by using the Friedman and Krishnan model [38] of overlap of solute hydration spheres. According to this model, the superposition of the hydration spheres causes a decrease in the number of water molecules surrounding the solutes, which leads to their partial dehydration and, consequently, an increase in their apparent partial molar volume. This effect is greater as the concentration of both solutes increases. Positive values of the transfer volume indicate a predominance of hydrophilic interactions (between the -OH groups of the CD surface and the -OH and -NO_2 groups of 4-NP) over hydrophobic interactions (between the nonpolar -CH_2- groups of the CD and the 4-NP ring), which intensify as the concentration of 4-NP in the solution increases [34].

In the infinite dilution situation, the limiting value found, ΔV_ϕ^0, is also positive (= 10.99 cm^3 mol^{-1}). Remembering that at infinitesimal concentration the interactions between the solute molecules are practically non-existent, the observed transfer volume is the result of the interactions between the solute and the solvent molecules. The fact that this transfer volume has a positive value means that the hydrogen bond interactions between the hydrophilic groups of 4-NP and the water dipoles (which contribute to an increase in said volume) are predominant.

 doi:10.20944/preprints202511.0705.v1

2.2.2.2. Interaction Volumes and Intrinsic Volumes

The process of dissolving a solute in a solvent can be considered to occur in two stages: a first in which a cavity of sufficient size is opened in the solvent for the solute molecule to enter, and a second one in which the solute enters this cavity and solute-solvent interactions are established. On this basis, the standard molar volume can be expressed as the sum of several contributions, as shown in the following equation [39]:

$$V_2^\circ = V_{intr} + V_T + V_{inter} + RT\kappa_{T0} \quad (10)$$

where V_{intr} is the intrinsic volume of the solute, V_T is a contribution related to the effects of packaging (corresponding to the empty space surrounding the solute molecule, caused by the thermal motion of solute and solvent molecules), V_{inter} is the interaction volume related to the solute-solvent interactions, while in the last term κ_{T0} is the isothermal compressibility of the solvent, R is the universal gas constant and T is the temperature in Kelvin. This last term is related to the volume effects of molecular motions [39] and since its contribution is small compared to the other terms, it can usually be ignored [40]. Since the terms $V_T + V_{inter}$ both depend on the solute-solvent interactions, it is possible to group them into a single term V_I. Finally, V_{intr} of solute can be identified with the Van der Waals volume V_W. According to the above, equation (10) can be reduced to:

$$V_2^\circ = V_w + V_I \quad (11)$$

If this equation is applied to the systems (4-NP + water) and (2-HP-β-CD + water), since the V_2° values are known and V_W values can be estimated theoretically, it is possible to calculate the V_I values. For this purpose, the V_W values for (4-NP) and (2-HP-β-CD) were calculated using Winmostar, after geometry optimization by MOPAC using a semi-empirical method. In the case of the complexes formed, the data obtained by H^1 NMR allow to know which protons are being affected and how the guest enters the host cavity. In this way, the architecture of the complex can be proposed, and the host-guest interactions analyzed. Table 6 shows the values of V_2°, V_W and V_I for (4-NP+water) and (2-HP-β-CD+water) systems:

Table 6. Values of V_2°, V_W and V_I for the systems (4-NP + water) and (2-HP-β-CD + water) at T = 298.15 K and P = 101.3 kPa.

	V_2° / ($cm^3 \cdot mol^{-1}$)	V_W / ($cm^3 \cdot mol^{-1}$)	V_I / ($cm^3 \cdot mol^{-1}$)
4-nitrophenol	94.83	67.35	27.48
2-HP-β-cyclodextrin	849.44	719.39	130.05

Standard uncertainties are $u_r(V_\phi)$ = 0.002 (max), $u(T)$ = 0.01K, $u(P)$ = 1 kPa.

For 4-NP in water the interactions that can be expected are due to the hydrogen bond between its hydroxyl group and the water molecules. The nitro group is a weak hydrogen bond acceptor because the N-O bond is non polar enough. However, these interactions are sufficient to make this molecule moderately soluble in water, which contributes to its problematic nature [41]. Meanwhile, for 2-HP-β-cyclodextrin in water, it is possible to think about the formation of hydrogen bond with the hydroxyl groups on the outside of the cyclodextrin, which is hydrophilic, not with its inside because its cavity is hydrophobic. Water can form hydrogen bonds with the cyclodextrin either through the upper rim of the cone, with the secondary hydroxyl groups, or through the lower rim of the cone, with the primary hydroxyl groups of the cyclodextrin. The interactions that can be expected for the complex in water when the 4-NP is placed inside the hydrophobic cavity of the cyclodextrin can be due to hydrophobic interactions between the aromatic ring of the phenol and the hydrophobic inside of the cyclodextrin (H-C, C-C and glycosidic bonds) and Van Der Waals interactions. Both at the bottom and top of the cyclodextrin, interactions with the hydroxyl group of the phenol can be expected (depending on how it enters, see NMR). While outside the complex there may be hydrogen

 doi:10.20944/preprints202511.0705.v1

bonding interactions between the hydroxyl groups of the cyclodextrins and water, this is what increases the solubility of (4-NP) complexed with the cyclodextrin compared to the solubility of (4-NP) when it is alone in water. Some of these interactions were confirmed by ^{1}H-NMR, which revealed that strong interactions occurs between the OH functional group of (4-NP) and the polar cavity of (2-HP-β-CD), possibly through hydrogen-bonding interactions. Figure 5 schematizes the complex formed.

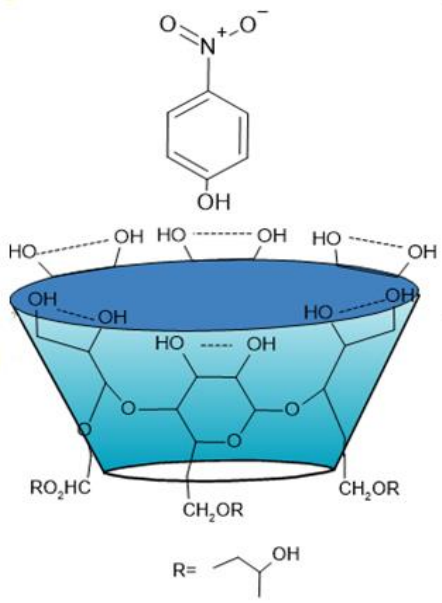

Figure 5. Scheme of the entry of (4-NP) into the cavity of (2-HP-β-CD).

3. Materials and Methods

3.1. Materials

2-hydroxypropyl-β-cyclodextrin (2-HP-β-CD; Sigma-Aldrich, Darmstadt, Germany; average molar mass M ≈ 1380 g mol^{-1}, mass fraction purity ≥ 0.98, water content of 10.3% mass fraction, by Karl-Fisher analysis reported by the supplier) and 4-nitrophenol (4-NP; Panreac Química S.L.U., Castellar del Vallès, Spain; molar mass M = 139.11 g mol^{-1}, purity 99%) were used as received. These chemicals were stored in a desiccator over silica gel. Milli Q® grade water (from EQ 7000 Ultrapure Water Purification System-Merck Millipore, Darmsdadt, Germany; $\kappa = 5.6 \times 10^{-8}$ S cm^{-1}) was used as solvent; it was degassed before use (Table 7). Solutions were prepared by direct weighing of their components by using a Sartorius analytical balance (Sartorius AG, Gottingen, Germany) with an accuracy of 1×10^{-5} g in the range of interest. Both the purity and the water content of the chemicals used were taken into consideration to calculate the molal concentration of the solutions. The solution was degassed before the experiment was run.

Table 7. Sample description.

Chemical Name	Source	CAS Number	Mass Fraction Purity [1]
2-HP-β-CD	Sigma-Aldrich (water content 10.3 % mass fraction)[2]	128446-35-5	>0.98
4-NP	Panreac Química S.L.U	100-02-7	0.99
Water	Millipore-Q water ($\kappa = 5.6 \times 10^{-8}$ S cm^{-1})		

 doi:10.20944/preprints202511.0705.v1

[1] Information provided by the supplier; [2] Upon receipt of the chemical, its water content was checked using Karl-Fischer analysis; these checks were performed periodically throughout the course of this work. Both purity and water content of the chemicals were taken into account to determine the concentration of the work solutions.

3.2. UV-Visible Analysis

UV-Visible analyses were carried out on a Lambda 365 Perkin-Elmer spectrometer (Perkin-Elmer, Shelton, CT, USA). Detection was performed in the range of 200-800 nm. UV-Vis absorption spectra were measured in water. Stock solutions, 1 mM of (2-HP-*β*-CD) and 10 mM of (4-NP), were prepared in H_2O.

3.3. ^{1}H-NMR Analysis

^{1}H-NMR spectra were recorded in D_2O at 400 MHz using a Bruker Avance 400 instrument (Bruker Scientific Instruments, Billerica, MA, USA). Chemical shifts are reported in ppm, using the residual solvent signal (D_2O) as a reference. A total of seven samples of mixtures of (4-NP) and (2-HP-β-CD) were prepared using a fixed amount of (2-HP-*β*-CD), (20 mg in 600 µL), and a solution of (4-NP) (0.3 M) until a 1:1 molar ratio was reached. The total volume of solution prepared was, in all cases, 700 µL. After each addition, the ^{1}H-NMR spectrum was recorded. The concentrations of the guest and host in the solution were corrected for each addition.

3.4. Density and Speed of Sound Measurements

Densities and speed of sound were measured with an Anton Paar DMA 5000 densimeter (Anton Paar Spain S.L.U., Madrid, Spain). The functioning of this instrument is based on the vibration, at a frequency of 3 MHz, of a U-tube containing the solution under study. The sensitivity of this equipment is 1×10^{-6} g·cm^{-3}, with a reproducibility of $\pm 5 \times 10^{-6}$ g·cm^{-3}, for density measurements, and 1×10^{-2} m·s^{-1}, with a reproducibility of $\pm 3 \times 10^{-2}$ m·s^{-1}, for measurements of the speed of sound through the working solution. This densitometer is equipped with a Peltier temperature control system that allows a stability better than ±0.005 degrees, over a temperature range of (0 to 90) °C and pressure range of (0-1.0) MPa. The instrument was verified, at the beginning and the end of each measurement session, using dry air and degassed ultrapure water (Milli-Q quality) at 293.15 K, according to the recommendations of the supplier.

The reported density data are the average of at least three independent measurements that were reproducible within 1×10^{-3} kg m^{-3}, with an uncertainty of 0.150 kg m^{-3}, according to NIST [42].

4. Conclusions

Based on the analysis of UV-Vis spectra, as well as the results of FT-IR and ^{1}H-NMR spectroscopy, the complexing capacity of (2-hydroxypropyl)-β-cyclodextrin with 4-nitrophenol was determined. Specifically, the results observed by ^{1}H-NMR suggested that the hydroxyl group of 4-nitrophenol could enter the cyclodextrin cavity and possibly be stabilized inside by hydrogen bond-type interactions.

On the other hand, based on experimental measurements of density and speed of sound, values of the apparent partial molar volume, V_ϕ, and the apparent partial molar adiabatic compressibility, κ_ϕ, were obtained for aqueous solutions of (4-NP), (2-HP-*β*-CD) and of the complex {(4-NP) + (2-HP-*β*-CD)} and their behavior analyzed as a function of the concentration, at 298.15 K.

Furthermore, partial molar volumes of transfer, ΔV_ϕ, for 4-NP from water to the different (2-HP-*β*-CD + water) mixed solvents were calculated, along with the value corresponding to the infinite dilution condition. The positive value found for this limiting transfer parameter confirms that hydrogen bonding interactions between the hydrophilic groups of 4-NP and the water dipoles are predominant.

Finally, from the standard molar volume values found, both the interaction and the intrinsic volumes were estimated and interpreted in terms of the different hydrogen bonds that can be

 doi:10.20944/preprints202511.0705.v1

established between the hydroxyl group of 4-NP, the hydroxyl groups of the cyclodextrin and the water molecules.

Supplementary Materials: The following supporting information can be downloaded at the website of this paper posted on Preprints.org.

Author Contributions: Conceptualization, M.M. and M.A.E; methodology, ESE, DMG and MM; software, ESE and MAE; validation, MAE and CMR.; formal analysis, M.M., CMR and M.A.E. ; investigation, MAE, ESE, MM, CMR and DMG; resources, M.M.; data curation, MM, ESE and DMG; writing—original draft preparation, MM, ESE and DMG; writing—review and editing, M.M., CMR and M.A.E.; supervision, M.M. and M.A.E.; project administration, MAE. All authors have read and agreed to the published version of the manuscript.

Funding: This research received no external funding.

Institutional Review Board Statement: Not applicable.

Informed Consent Statement: Not applicable.

Data Availability Statement: The data obtained is presented in the article.

Acknowledgments: The authors would like to thank the Universidad Nacional de Colombia-Sede Bogotá and the Catholic University of Ávila, Spain.

Conflicts of Interest: The authors declare no conflicts of interest.

References

1. Ruzgar, A.; Karatas, Y.; Gülcan, M. Synthesis and characterization of Pd nanoparticles supported over hydroxyapatite nanospheres for potential application as a promising catalyst for nitrophenol reduction. *Heliyon* **2023**, *9*, e21517. https://doi.org/10.1016/ j.heliyon.2023.e21517.
2. Rika, Y.; Cantik, C. D.; Devi, A.; Achmad, B.; Aminah, U.; Adid, D.; Jeong-Myeong, H. Comparison study of the effects of different synthesis methods towards Ag2O/TiO2 nanowires morphology and catalytic activity on the 4-nitrophenol reduction reaction. *Nano-structures & nano-objects* **2023**, *36*,101042. https://doi.org/10.1016/j.nanoso.2023.101042
3. Pandey, S.; Singh, A.; Kumar, A.; Tyagi, I.; Karri, R.R.; Gaur, R.; Javadian, H.; Verma, M. Photocatalytic degradation of noxious p-nitrophenol using hydrothermally synthesized stannous and zinc oxide catalysts, *Physics and Chemistry of the Earth* **2024**, *133*, 10351. https://doi.org/10.1016/j.pce.2023.103512
4. Dutt, S.; Singh, A.; Mahadeva, R.; Sundramoorthy, A.K.; Gupta, V.; Arya, S. A reduced graphene oxide-based electrochemical sensing and eco-friendly 4-nitrophenol degradation. Diamond & related materials **2024**, *141*, 110554. https://doi.org/10.1016/j.diamond.2023.110554
5. Guo, Z.; Hu, X.; Sun, W.; Peng, X.; Fu, Y.; Liu, K.; Liu, F.; Meng, H.; Zhu, Y.; Zhang, G.; Wang, X.; Xue, L.; Wang, J.; Wang, X.; Peng, P.; Bi, X. Mixing state and influence factors controlling diurnal variation of particulate nitrophenol compounds at a suburban area in northern China, *Environmental pollution* **2024**, 123368. https://doi.org/10.1016/j.envpol.2024.123368
6. Deng, P.; Zeng, Y.; Wei, Y.; Li, J.; Yao, L.; Liu, X.; Ding, J.; Li, K.; He, Q. An efficient electrochemical sensor based on multi-walled carbon nanotubes functionalized with polyethylenimine for simultaneous determination of o-nitrophenol and p-nitrophenol. *Microchemical Journal* **2023**, *186*, 108340. https://doi.org/10.1016/j.microc.2022.108340
7. Bharadwaj, K.K.; Rabha, B.; Pati, S., Choudhury, B.K.; Sarkar, T.; Godoi, S.K.; Kakati, N.; Baishya, D.; Kari, Z.A.; Edinur, H.A. Green synthesis of silver nanoparticles using diospyros malabarica fruit extrac and assessment of their antimicrobial, anticancer and catalytic reduction of 4-nitrophenol (4-NP). *Nanomaterials* **2021**, *11* (8), 1999. https://doi.org/10.1016/j.pce.2023.103512
8. Jacob, J.A.E.; Antony, R.; Jebakumar, D.S.I. Synergistic effect of silver nanoparticle-embedded calcite-rich biochar derived from Tamarindus indica bark on 4-nitrophenol reduction. *Chemosphere* **2024**, *349*, 140765. https://doi.org/10.1016/j.chemosphere.2023.140765

 doi:10.20944/preprints202511.0705.v1

9. Karri, R.R.; Ravindran, G.; Dehghani, M.H. Wastewater—Sources, Toxicity, and Their Consequences to Human Health. Soft Computing Techniques in Solid Waste and Wastewater Management 1 (2021) 3-33. https://doi.org/10.1016/B978-0-12-824463-0.00001-X
10. Yarmohammadi, F.; Karimi; G. 4-Nitrophenol. *Encyclopedia of toxicology (fourth edition)* **2024**, *6*, 923-927. https://doi.org/10.1016/B978-0-12-824315-2.00052-X
11. Giribabu, K.; Haldorai, Y.; Rethinasabapathy, M.; Jang, S-Ch.; Ranganathan Suresh, R.; Cho, W-S.; Han, Y-K.; Roh, Ch.; Huh, Y.S.; Narayanan, V. Glassy carbon electrode modified with poly(methyl orange) as an electrochemical platform for the determination of 4-nitrophenol at nanomolar levels. Current Applied Physics **2017**, 17 (8), 1114-1119. https://doi.org/10.1016/j.cap.2017.04.016
12. Hryniewicz, B.; Orth, E.; Vidotti, M. Enzymeless PEDOT-based electrochemical sensor for the detection of nitrophenols and organophosphates. *Sensors and Actuators B: Chemical* **2018**, *257*, 570-578. https://doi.org/10.1016/j.snb.2017.10.162
13. Luo, S.; Zeng, Y.; Huang, X. Preparation of an imprinted monolith for field simultaneously selective separation and enrichment of nitrophenols and lead (II) ion in water samples. *Separation and Purification Technology* **2024**, *337*, 126109. https://doi.org/10.1016/j.seppur.2023.126109
14. Pal, M.; Shankar, K.; Baruah, J. Study on the interactions of nitrophenols with bis-8-hydroxyquinolinium zinc-2,6-pyridinedicarboxylate. *Inorganica Chimica Acta* **2019**, *489*, 204-210. https://doi.org/10.1016/j.ica.2019.02.029
15. Ferhat, M.F.; Ghezzar, M.R.; Smail, B.; Guyon, C.; Ognier, S.; Addou, A. Conception of a novel spray tower plasma-reactor in a spatial post-discharge configuration: Pollutans remote treatment. *J. Hazardous Materials* **2017**, *321*, 661-671. http://dx.doi.org/10.1016/j.jhazmat.2016.09.052
16. Tugba, E.; Tekintas, K.; Bekircan, O.; Biyiklioglu, Z. Enhancing the photocatalytic performance of Co(II) and Cu (II) phthalocyanine by containing 1,3,4 thiadiazole groups in 4-nitrophenol oxidation reaction. *Inorganica Chimica Acta* **2023**, *547*, 121342. https://doi.org/10.1016/j.ica.2022.121342
17. Sajjan, V.; Aralekallu, S.; Nemakal, M.; Palanna, M.; Keshavananda, P.; Koodlur, L. Nanomolar detection of 4-nitrophenol using Schiff-base phthalocyanine. *Microchemical Journal* **2021**, *164*, 105980. https://doi.org/10.1016/j.microc.2021.105980
18. Moro, P.; Donzello, M. P.; Ercolani, C.; Monacelli, F.; Moretii, G. Tetrakis-2,3-[5,6-di-(2-pyridyl)-pyrazino] porphyrazine, and its Cu(II) complex as sensitizers in the TiO2-based photo -degradation of 4-nitrophenol. *J. Photochemistry and Photobiology A: Chemistry* **2011**; *220*, 77-83. https://doi:10.1016/j.jphotochem.2011.03.023
19. Guergueb, M.; Nasri, S.; Brahmi, J.; Al-Ghemdi, Y.; Loiseau, F.; Molton, F.; Roisnel, T.; Guerineau, V.; Nasri, H. Spectroscopic characterization, X-ray molecular structures and cyclic voltammetry study of two (piperazine) cobalt (II) meso-arylporphyin complexes. Application as a catalyst for the degradation of 4-nitrophenol. *Polyhedron* **2021**, *209*, 115468. https://doi.org/10.1016/j.poly.2021.115468
20. Galindres D.M.; Espitia-Galindo, N.; Valente, A.J.M.; Sofio, S.P.C.; Rodrigo, M.M.; Cabral, A.M.T.D.P.V.; Esteso, M.A.; Zapata-Rivera, J.; Vargas, E.F.; Ribeiro, A.C.F. Interactions of Sodium Salicylate with β-Cyclodextrin and an Anionic Resorcin[4]arene: Mutual Diffusion Coefficients and Computational Study. *Int. J. Mol. Sci.* **2023**, *24*, 3921. https://doi.org/10.3390/ijms24043921
21. Xiao, Z.; Yu, P.; Sun, P.; Kang, Y.; Niu, Y.; She, Y.; Zhao, D. Inclusion complexes of β-cyclodextrin with isomeric ester aroma compounds: Preparation, characterization, mechanism study, and controlled release. *Carbohydrate Polymers* **2024**, *333*, 121977. https://doi.org/10.1016/j.carbpol.2024.121977
22. Bezerra, F.M.; Lis, M.J.; Firmino, H.B.; Dias da Silva, J.G.; Valle, R.C.S.C.; Valle, J.A.B.; Scacchetti, F.A.P.; Tessaro, A.L. The Role Of *β*-Cyclodextrin In The Textile Industry—Review. *Molecules* **2020**, *25*, 3624. https://doi.org/10.3390/molecules25163624
23. Raju, N.; Benjakul, S. Use of beta cyclodextrin to remove cholesterol and increase astaxanthin content in shrimp oil. *Eur. J. Lipid Sci. Technol.* **2019**, *122*, 1900242. https://doi.org/10.1002/ejlt.201900242
24. Paul, P.; Gupta, U.; Kumar, R.; Munagalasetty, S.; Prasad, H.; Nair, R.; Mahajan, S.; Maji, I.; Aalhate, M.; Bhandary, V.; Kumar, S.; Kumar, P. Fabrication of β-cyclodextrin and 2-hydroxypropyl-β-cyclodextrin inclusion complexes of Palbociclib: Physicochemical characterization, solubility enhancement, in silicio studies, in vitro assessment in MDA-MB-231 cell line. *J. Mol. Liquids* **2024**, *399*, 124458. https://doi.org/10.1016/j.molliq.2024.124458

 doi:10.20944/preprints202511.0705.v1

25. Burakowski A., J. Glinski. Hydratation munbers of nonelectrolytes from acoustic methods, Chem. Rev. 112 (2012) 2059-2081. https://doi.org/10.1021/cr2000948
26. Vass, S.; Töröc, T.; Jákli, G.; Berecz, E. Sodium Akyl Sulfate Apparent Molar Volumes in Normal and Heavy Water: Connection with Micellar Structure, *J. Phys. Chem.* **1989**, *93*, 6553-6559. https://doi.org/10.1021/j100354a053
27. Pérez-Rodriguez, M.; Prieto, G.; Carlos, C.; Varela, L. M.; Sarmiento, F.; Mosquera, V. A comparative Study of the Determination of the Critical Micelle Concentration by Conductivity and Dielectric Constant Measurements. *Langmuir* **1998**, *14*, *16*, 4422-4426. https://doi.org/10.1021/la980296a
28. Savaroglu, G.; Genc, L. Determination of micelle formation of ketorolac tromethamine in aqueous media by acoustic measurements. *Thermochimica Acta* **2013**, *552*, 5-9. https://doi.org/10.1016/j.tca.2012.11.008
29. Redlich, O. Molal volumes of solute, IV. *J. Phys. Chem.* **1940**, *44* (5), 619–629. https://doi.org/10.1021/j150401a008
30. Patil, P.P.; Shaikh, V.R.; Patil, P.D.; Borse, A.U.; Patil, K.J. Volumetric, isentropic compressibility and viscosity coefficient studies of binary solutions involving amides as a solute in aqueous and CCl4 solvent systems at 298.15 K. *J. Mol. Liquids* **2018**, *264*, 223-232, https://doi.org/10.1016/j.molliq.2018.05.062
31. Jahagirdar, D.V.; Arbad, B.R.; Walvekar, A.A.; Shankarwar, A.G. Studies in partial molar volumes, partial molar compressibilities and viscosity B-coefficients of caffeine in water at four temperatures. *J. Mol. Liquids* **2000**, *85*, 361-373. https://doi.org/10.1016/S0167-7322(00)89019-4
32. Duman, O.; Ayranci, E. Apparent molar volumes and isentropic compressibilities of benzyltrialkylammonium chlorides in water at (293.15, 303.15, 313.15, 323.15 and 333.15) K. *J. Chem. Thermodyn*. **2009**, *41*, 911-915. https://doi.org/10.1016/j.jct.2009.03.004
33. Blanco, L.H.; Salamanca, Y.P.; Vargas, E.F. Apparent molal volumes and expansibilities of Tetraalkylammonium Bromide in dilute aqueous solutions. *J. Chem. Eng. Data* **2008**, *53*, 2770-2776. https://doi.org/10.1021/je800329m
34. Santos, C. I.A.V.; Teijeiro, C.; Ribeiro, A. C.F.; Rodrigues, D. F.S.L.; Romero, C. M.; Esteso, M. A. Drug delivery systems: Study of inclusion complex formation for ternary caffeine–β-cyclodextrin–water mixtures from apparent molar volume values at 298.15 K and 310.15 K. *J. Mol. Liquids* **2016**, *223*, 209–216. http://dx.doi.org/10.1016/j.molliq.2016.08.035
35. Sarkar, A.; Pandit, B.K.; Acharjee, K.; Sinha, B. Volumetric and Viscometric Behavior of Ferrous Sulfate in Aqueous Lactose Solutions at Different Temperatures. *Indian J. Advances in Chemical Science* **2015**, *3*(3), 219-229.
36. Desnoyers, J.E. Structural effects in aqueous solutions: a thermodynamic approach**.** *Pure Appl. Chem*. **1982**, *54*, 1469-1478. http://dx.doi.org/10.1351/pac198254081469
37. Ali, A.; Shahjahan, S. Volumetric, viscometric and refractive index behavior of some α-amino acids in aqueous tetrapropylammonium bromide at different temperatures. *J. Iran. Chem. Soc*. **2006**, *3* (4), 340-350. https://doi.org/10.1007/BF03245957
38. Friedman, H. L.; Krishnan, C. V. (1973). Thermodynamics of Ionic Hydration. In: Franks, F. (ed.) *Water: A Comprehensive Treatise*, Vol. 3. Aqueous Solutions of Simple Electrolytes. Plenum Press, New York. Chp. 1, pp. 1-118. https://doi.org/10.1007/978-1-4684-2955-8_1
39. Likhodi, O.; Chalikian, T.V. Partial molar volumes and adiabatic compressibilities of a series of aliphatic amino acids and oligoglycines in D_2O, *J. Am. Chem. Soc.* **1999**, *121*, 1156–1163. https://doi.org/10.1021/ja983127
40. Riveros, D.C.; Hefter, G.; Vargas, E. F. Thermodynamic evidence for nano-heterogeneity in solutions of the macrocycle C-butylresorcin[4]arene in non-aqueous solvents. *J. Chem. Thermodynamics* **2018**, *125*, 250-256. https://doi.org/10.1016/j.jct.2018.06.006
41. Badamasi, H.; Naeem, Z.; Antoniolli, G.; Praveen, A.; Ademola, A.; Shina, I.; Duriminiya, N.; Salman, M. A review of recent advances in green abd sustainable technologies for removing 4-nitrophenol from the water and wastewater. *Sustain. Chem. Pharm.* **2025**, *43*, 10186. https://doi.org/10.1016/j.scp.2024.101867
42. Taylor, B.N.; Kuyatt, C.E. Guidelines for Evaluating and Expressing the Uncertainty of NIST Measurement Results; NIST Technical Note 1297; National Institute of Standards and Technology: Gaithersburg, MD, USA, 1994.

 doi:10.20944/preprints202511.0705.v1